Design of autostereoscopic two-view 3D that uses the spherical concave surface and the parallax barrier

Hyungki Hong (SID Member)

Abstract **—** Autostereoscopic display where circular concave display was used was investigated in case of the parallax barrier and two-view 3D. Equation of the barrier pitch of the parallax barrier was derived that depended on the radius of the curved display. Trajectories of the rays coming from the curved display through the parallax barrier were calculated. Calculated distribution of ray trajectories for the autostereoscopic display using curved display showed trends similar to those for the flat display.

Keywords — *autostereoscopic, 3D, curved, concave.*

DOI # 10.1002/jsid.228

1 Introduction

Nowadays, 3D displays using special eyeglasses had been widely adapted for applications such as in TV.[1] And autostereoscopic 3D, where the naked eye of a user could perceive the stereoscopic image, had been also researched as well.[2–7] Control of ray directions were key factors designing the autostereoscopic display and the optical element such as the parallax barrier or the lenticular lens sheet had been used to control the direction of the ray.[2–7]

Curved displays using organic light-emitting diode or liquid crystal display had been reported.[8–12] As the distributions of the direction of the rays coming out from the curved surface of the display were different from those of the flat surface, the curved shape of the display surface should be considered in designing autostereoscopic 3D display.

For this purpose, the relation between the shape of the display surface and the ray direction was investigated. In the design of the autostereoscopic two-view 3D using the parallax barrier, this relation was used to determine the parameters of the parallax barrier. Using these parameters of the parallax barrier, trajectories of the rays coming out from the autostereoscopic 3D display were calculated and compared with those of the case for the display of the flat surface.

2 Methods

In this paper, autostereoscopic two-view 3D using parallax barrier was selected as an example for the analysis.

Figure 1 illustrates the configuration where a display of the flat surface was used for the autostereoscopic display. Parallax barrier consisted of the transparent and non-transparent regions. The thickness of the light-absorbing layer, which was located at the non-transparent region, was generally much thinner than the thickness of the substrates, which composed the parallax barrier or the display. So the position of the light-absorbing layer inside the parallax barrier was considered as illustrated in Fig. 1. In Fig. 1, the distance from the pixel of the display to the light-absorbing layer of the parallax barrier and the distance from the light-absorbing layer to the air were denoted as a and b. The values of a and b and the pitch of the parallax barrier should be determined such that the light rays passing through the parallax barrier could make the viewing zone of autostereoscopic 3D. In the example in Fig. 1, the relative position between the pixels and the transparent region of the parallax barrier were selected such that among the rays coming out from the center of pixel $P_{(n)\mathrm{C}}$, rays normal to the display surface passed through the transparent region of the parallax barrier. In case of the rays coming out from other pixels such as $P_{(n+1)\mathrm{C}}$, $P_{(n-1)\mathrm{C}}$, rays normal to the display surface were blocked by the non-transparent region of the parallax barrier. As the distribution of the ray trajectories coming from each pixel became different owing to the parallax barrier, ray trajectories for more than one pixels need to be considered to investigate the ray distribution of the autostereoscopic 3D. Hence, five pixels were considered for two-view 3D. In case of autostereoscopic two-view 3D, light rays from the pixels of the notation of even or odd number had to be observed by only one eye of a user at the viewing distance. If the view number of the autostereoscopic display was larger than 2, more pixels need to be considered.

The value of a of the parallax barrier in Fig. 1 was determined by the following equation. Once viewing distance D and the distance between the adjacent viewing zones were given, angle θ_2 between the adjacent viewing zones in Fig. 1 can be represented as in Eq. (1a).[2,4]

$$\tan\theta_2 = E_v/D \tag{1a}$$

Received 02/28/14; accepted 07/01/14.

The author is with the Department of Optometry, Seoul National University of Science and Technology, Seoul, Korea; email: hyungki.hong@snut.ac.kr.

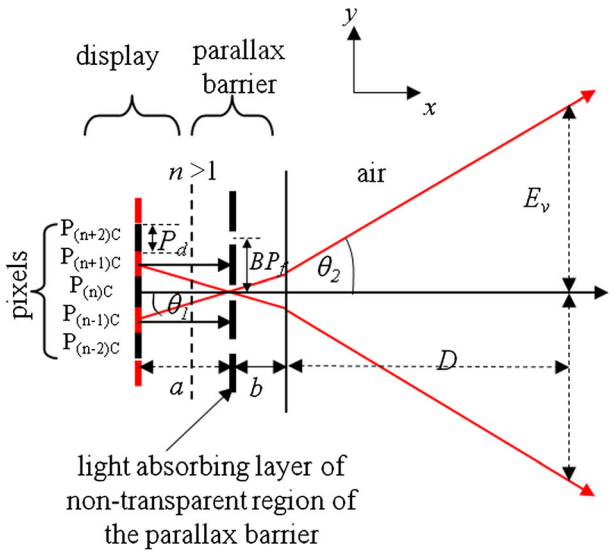

FIGURE 1 — Schematics of autostereoscopic two-view display using the parallax barrier and the flat surface. E_v is the distance between the viewing zones for the left and right eyes. *D*, *b*, and *a* represent the distance from the user to the substrate of the parallax barrier, the distance between the air and the light-absorbing layer of the non-transparent region of the parallax barrier, and the distance between the light-absorbing layer and the display pixel, respectively. $P_{(n)C}$ represents the pixel on the display where integer *n* is used to represent the different pixels. P_d and BP_f represent the pixel pitch of the display and the parallax barrier pitch, respectively.

E_v represents the distance between the adjacent viewing zones. From Snell's equation, angle θ_1 from the transparent region of the parallax barrier to the center of pixel $P_{(n-1)C}$, which was located next to pixel $P_{(n)C}$, can be represented as in Eq. (1b).

$$\theta_1 = \sin^{-1}\left(\frac{\sin\theta_2}{n}\right) \tag{1b}$$

From angle θ_1, *a* of the parallax barrier can be determined as in Eq. 1c. P_d represents the pixel pitch of the display.

$$a = P_d \tan\theta_1 = P_d \tan\left(\sin^{-1}\left(\frac{\sin\theta_2}{n}\right)\right) \tag{1c}$$

For autostereoscopic 3D with the flat surface, the parallax barrier consisted of the transparent and non-transparent regions, which were repeated by the spatial period of the barrier pitch. The size of the barrier pitch had been determined by Eq. (2).[2,4] Subscript *f* was used to represent the flat surface.

$$BP_f = \frac{2}{1/P_d + 1/E_v} \tag{2}$$

At the viewing zones of autostereoscopic 3D, each eye of a user should only observe lights coming from the pixels corresponding to the specific view. Hence, the trajectories of the rays coming out from the pixels corresponding to the specific view should intersect at the viewing zone of that view. Therefore, the viewing zone can be approximately determined from the positions of these intersections. Trajectories of rays coming from the center and the horizontal left/right edges of the display were considered as illustrated in Fig. 2.[6,7]

In Fig. 1, the position of pixel $P_{(n)C}$ at the display center was selected such that among the rays coming out from the center of pixel $P_{(n)C}$, rays normal to the display surface passed through the transparent region of the parallax barrier. In Fig. 2, $P_{(n)L}$ and $P_{(n)R}$ represent pixels that were located far from the center of the display. *M* was the number of pixels between the positions of $P_{(n)C}$ and $P_{(n)R}$ or $P_{(n)L}$. D_L represents the distance from $P_{(n)C}$ to $P_{(n)R}$ or $P_{(n)L}$. If pixel $P_{(n)C}$, $P_{(n)R}$, and $P_{(n)L}$ corresponded to the same view, *M* should be an even number for two-view 3D. From Eq. (2) of the barrier pitch, the size of barrier pitch was always smaller than twice the pixel pitch. So the relative position between the pixel corresponding to the specific view and the transparent region of the parallax barrier became different for the different positions of the display. Hence, the center of pixel $P_{(n)R}$ at the right edge of the display and the transparent region of the parallax barrier were not aligned anymore. In case of the rays coming from $P_{(n)R}$, the rays normal to the display surface did not reach the user as illustrated in Fig. 2. Only rays of angle ϕ_1 coming from $P_{(n)R}$ passed through the transparent region of the parallax barrier and could reach the user. In Fig. 2, the *xy*-coordinate system was selected where the *x*-axis represents the direction normal to the surface at the center of the display and the *y*-axis is parallel to the horizontal direction

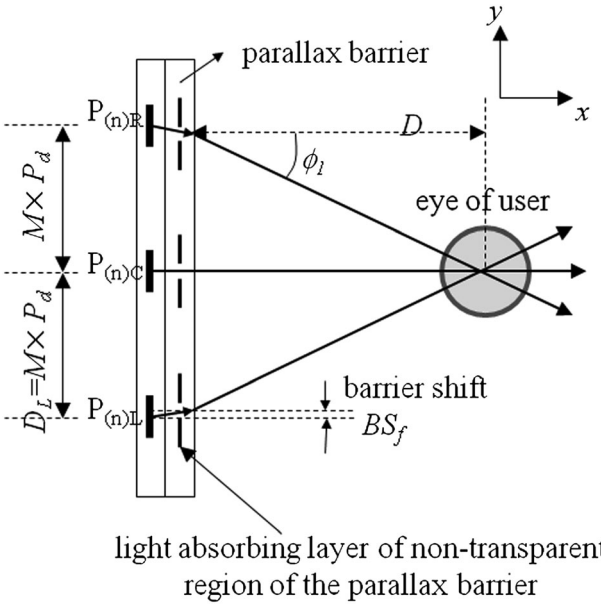

FIGURE 2 — Ray directions passing through the parallax barrier at the center and the left and right edges of the autostereoscopic two-view display of the flat surface in the *xy*-coordinate system where the *x*-axis is parallel to the direction normal to the surface at the center of the display and the *y*-axis is parallel to the horizontal direction of the user. P_d represents the pixel pitch of the display. *M* represents the number of pixels between pixels of $P_{(n)C}$ and $P_{(n)R}$ or $P_{(n)L}$. User was located at viewing distance *D* from the 3D display.

of the user. The situation was similar for pixel $P_{(n)\mathrm{L}}$ located at the left edge of the display. Angle ϕ_1 was related to viewing distance D as shown in Eq. (3).

$$\phi_1 = \tan^{-1}(D_L/D) \tag{3}$$

In Figs 1 and 2, the spatial difference between the transparent region of the parallax barrier and the center of pixel $P_{(n)\mathrm{C}}$ was selected as zero. Barrier shift was defined as the spatial difference between the transparent region of the parallax barrier and the center of pixel $P_{(n)\mathrm{L}}$ or $P_{(n)\mathrm{R}}$. For 3D using the display of the flat surface, the barrier shift can be represented as in Eq. (4).

$$BS_f = M\times\left(2P_d - BP_f\right) \tag{4}$$

Subscript f was used to represent the flat surface. As distance D_L became larger, barrier shift and angle ϕ_1 became larger accordingly.

As an example of the curved display, a circular concave display where radius R of the display was equal to viewing distance D of autostereoscopic 3D was considered as illustrated in Fig. 3. Radius R was defined as the curvature at the surface of the barrier substrate. C represents the center of the concave curvature. $P_{(n)\mathrm{C}}$, $P_{(n)\mathrm{R}}$, and $P_{(n)\mathrm{L}}$ represent the pixels that correspond to the same view of autostereoscopic two-view 3D. So rays from these pixels should reach one eye of a user at the viewing distance. If a user was located at the distance of R from the curved display, the viewing direction of the user was always normal to the surface of the display. Hence, only one eye of the user could observe the rays normal to the display surface among the rays coming out from the pixels of the display as illustrated in Fig. 3(a). So the transparent regions of the parallax barrier should be placed in the trajectories of these rays. This situation was different from that of the flat surface in Fig. 2 where the viewing direction of the user for a view was not always normal to the surface of the display. So the equation to determine the barrier pitch needs to be newly derived for the curved display.

If a user was located at the distance of R from the curved display, the barrier pitch could be determined from the ratio of two similar fan shapes as illustrated in Fig. 3(b).

Angle ϕ_{P} of these fan shapes was the same. The distance from the center C to the light-absorbing layer was equal to the radius $(R+b)$ of one fan shape. The distance from the center C to the position of display pixels was equal to the radius $(R+a+b)$ of the other fan shape. Hence, the following equation was derived from the size of these similar fan shapes.

$$BP_r : 2P_d = (R+b) : (R+a+b) \tag{5a}$$

From this relation, the barrier pitch BP_r was determined as in Eq. (5b).

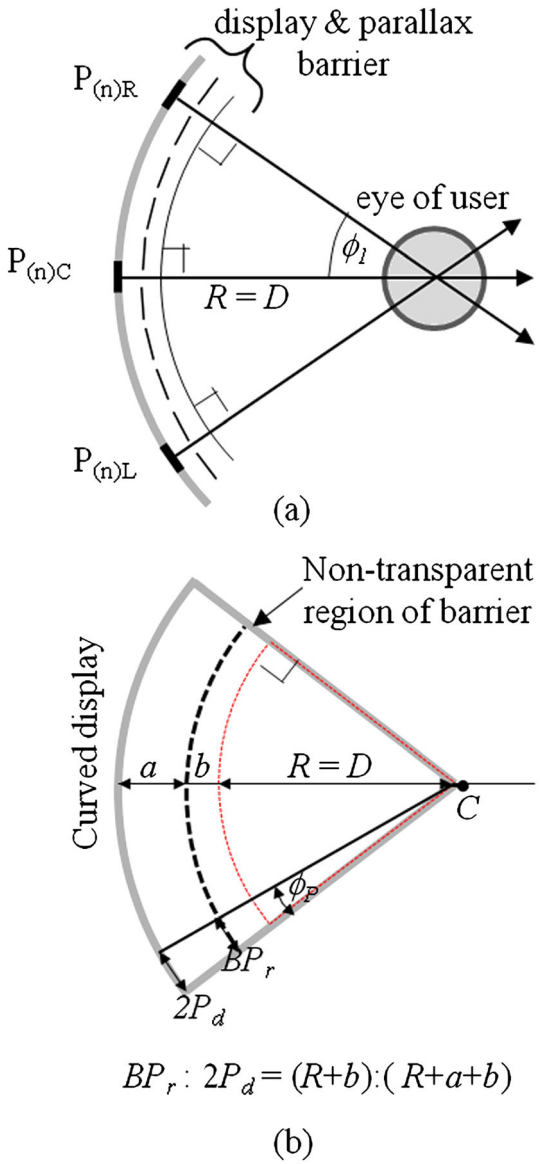

FIGURE 3 — Curved display where viewing distance D was equal to radius R of the concave curvature. User was located at the center C of the concave curvature. (a) Ray directions passing through the parallax barrier at the center and the left and right edges of the display. User can only observe the rays normal to the surface. (b) Determination of the barrier pitch BP_r from the similar shape of two fan shapes when $D=R$. Thick gray line and thick dotted line represent two fan shapes.

$$BP_r = 2P_d\frac{R+b}{R+b+a} \tag{5b}$$

Subscript r was used to represent the condition where radius R of the curved display was equal to viewing distance D. Compared with Eq. (2), Eq. (5b) was dependent on radius R and was independent of E_v, which was the distance between the adjacent viewing zones.

As another example of the curved display, Fig. 4(a) illustrates the case that viewing distance D was not equal to radius R of the display. The xy-coordinate system in Fig. 4

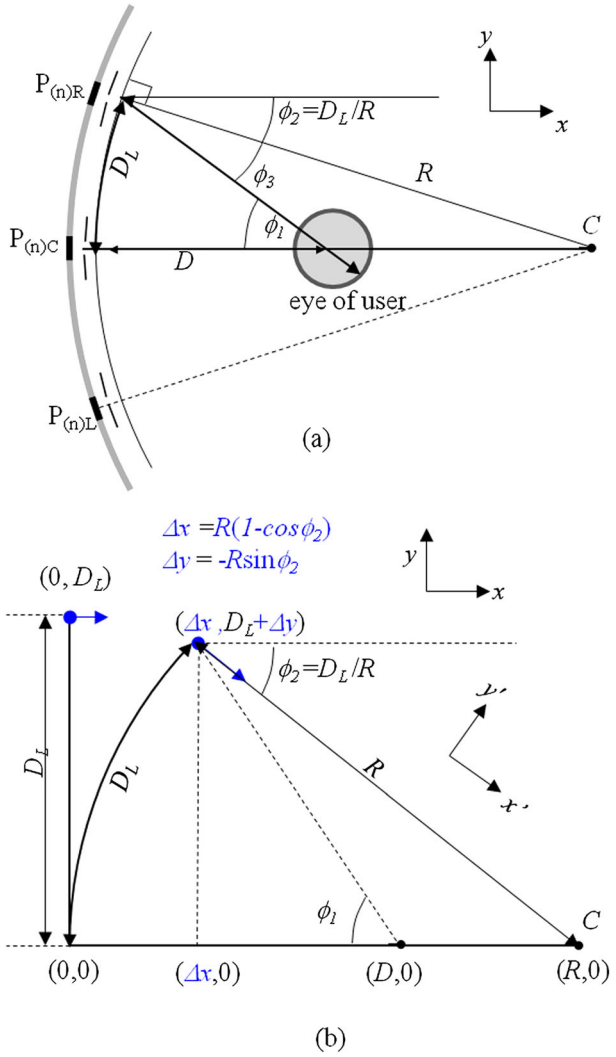

FIGURE 4 — Curved display where viewing distance D is not equal to radius R of the circular concave display. (a) Ray directions passing through the parallax barrier at the center and the left and right edges of the curved display. C represents the center of the concave curvature. (b) The xy-coordinate systems for the flat surface and the $x'y'$-coordinates systems for the curved surface at distance D_L from the center of the display. For the same distance D_L, positions on the flat and curved surfaces are different by the amount of (Δx, Δy) and angle ϕ_2. R and C represent the radius and the center of the concave curvature.

(a) is the same as the xy-coordinate system defined in Fig. 2. $P_{(n)C}$, $P_{(n)R}$, and $P_{(n)L}$ represent the pixels that correspond to the same view. It was assumed that among the rays coming from pixel $P_{(n)C}$, the rays normal to the display surface passed through the transparent region of the parallax barrier and reached the user similar to the case of Figs 2 and 3. However, except for the rays coming from pixel $P_{(n)C}$ at the center of the display, the rays normal to the display did not reach the user as illustrated in Fig. 4(a). In the xy-coordinate system, the angle between the x-axis and the normal direction at the position of pixel $P_{(n)R}$ far from the display center was defined as ϕ_2 where $\phi_2 = D_L/R$. ϕ_1 represents the angle of ray direction that reaches the user. ϕ_3 represents the angle between the direction normal to the surface and the direction toward the user. Equation 6a determines the relation of these angles of Fig. 4(a).

$$\phi_3 = \phi_1 - \phi_2 = \phi_1 - D_L/R \tag{6a}$$

As the direction normal to the surface was parallel to the x-axis only for the pixels located at the center of the display, the $x\,y$ -coordinate system was defined where the x -axis was normal to the display surface. Figure 4(b) represents the difference between the $x\,y$ -coordinate system of the curved surface to the xy-coordinate system defined in consideration of the user position. The differences of the positions and the direction normal to the flat or the curved surface of the display at the distance of D_L are illustrated in Fig. 4(b). Directions normal to the flat and the curved surface were different by angle ϕ_2. And positions at the distance of D_L were different by the amount of $(\Delta x,\ \Delta y) = (R(1-\cos\phi_2), -R\sin\phi_2)$. Angle ϕ_1 was determined as in Eq. (6b).

$$\phi_1 = \tan^{-1}\left(\frac{D_L + \Delta y}{D - \Delta x}\right) = \tan^{-1}\left(\frac{D_L - R\sin\phi_2}{D - R(1 - \cos\phi_2)}\right) \tag{6b}$$

Angle ϕ_1 of Eq. 6b was different from Eq. (3) of the flat surface. Yet, for the large R, angle ϕ_2 approaches zero, and the difference between Eq. (6b) and (3) also decreases.

If $\phi_3 = \phi_1 - \phi_2$ was not zero, the barrier pitch and barrier shift need to be adjusted such that rays at angle ϕ_3 could reach the user. Similar to the flat surface, barrier shift BS in the curved surface could be defined as the difference between the transparent region of the parallax barrier and the center of pixel $P_{(n)L}$ or $P_{(n)R}$ along the direction normal to the curved surface as illustrated in Fig. 5. The $x\,y$ -coordinate system

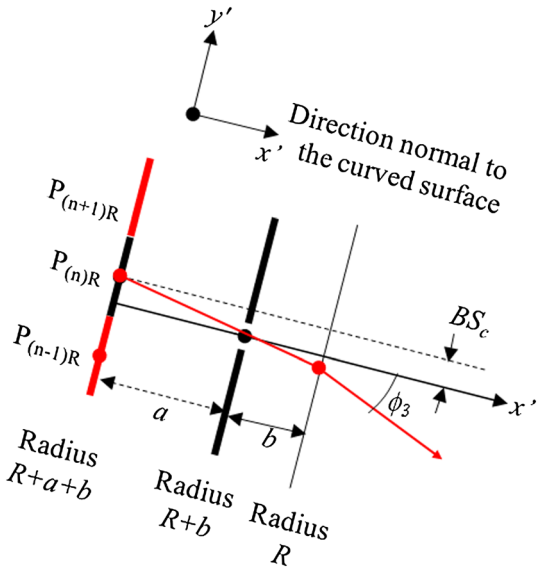

FIGURE 5 — Barrier shift BS_c of pixel $P_{(n)R}$ in the $x'y'$-coordinate system where the x'-axis was normal to the display surface in curved display and viewing distance D is not equal to radius R of the circular concave display.

was considered where the x-axis was normal to the display surface. This barrier shift was related to angle φ_3 in Eq. 7a. Subscript c represents the curved surface.

$$BS_c = a\tan\left(\sin^{-1}\left(\frac{\sin\phi_3}{n}\right)\right) \tag{7a}$$

The radii at the pixel position and the position of the light-absorbing layer are $(R+a+b)$ and $(R+b)$, respectively. When the difference of the radii was considered, barrier pitch BP_c can be written as in Eq. (7b).

$$BP_c = 2P_d\frac{R+b}{R+b+a} - \frac{BS_c}{M} \tag{7b}$$

If distance from the display surface to the user was equal to radius R, ϕ_3 was 0 and ϕ_1 was equal to ϕ_2 in Eq. (6a). As BS_c was 0, BP_c of Eq. (7b) became equal to BP_r of Eq. (5b). Hence, BP_r of Eq. (5b) for the curved surface of $R = D$ can be considered as the special case of Eq. (7b), which was derived for the curved surface of the arbitrary radius R. The equations of the barrier pitch and the barrier shift for the various shapes of the display surface are shown in Table 1.

Trajectories of the rays coming from the pixels through the parallax barrier were calculated to verify the barrier pitch of autostereoscopic 3D for the curved display to be correct. MATLAB™ was used for the calculation.[13] A display with diagonal size of 7 in., resolution of 1920 × 1080 pixels, and pixel pitch of 81 μm was considered as the display condition for the calculation. Refractive index of the display and the parallax barrier was selected as 1.5. The aperture ratio of the parallax barrier, which was defined as the size of the transparent region divided by the barrier pitch, was selected as 0.2. Viewing distance D was selected to be 400 mm in consideration of mobile application. The distance between the adjacent viewing zones was selected to be 65 mm, which was slightly larger than the pupillary distance.[14]

Figure 6(a) illustrates the schematics of the calculation for the pixels located at the center of the display in the $x\,y$-coordinate system where the x-axis was normal to the display surface.

TABLE 1 — Equations of barrier pitch and barrier shift for the flat and the curved surfaces.

	Barrier pitch	Barrier shift
Flat surface	$BP_f = \frac{2}{1/P_d+1/E_v}$	$BS_f = M\times(2P_dBP_f)/2$
Curved surface ($R=D$)	$BP_r = 2P_d\frac{R+b}{R+b+a}$	$BS_r = 0$
Curved surface ($R\neq D$)	$BP_c = 2P_d\frac{R+b}{R+b+a} - \frac{BS_c}{M}$	$BS_c = a\tan\left(\sin^{-1}\left(\frac{\sin\varphi_3}{n}\right)\right)$

Subscripts f, r, and c represent the conditions where display is flat, radius R is equal to distance D from the display to the user position, and R is not equal to D, respectively.

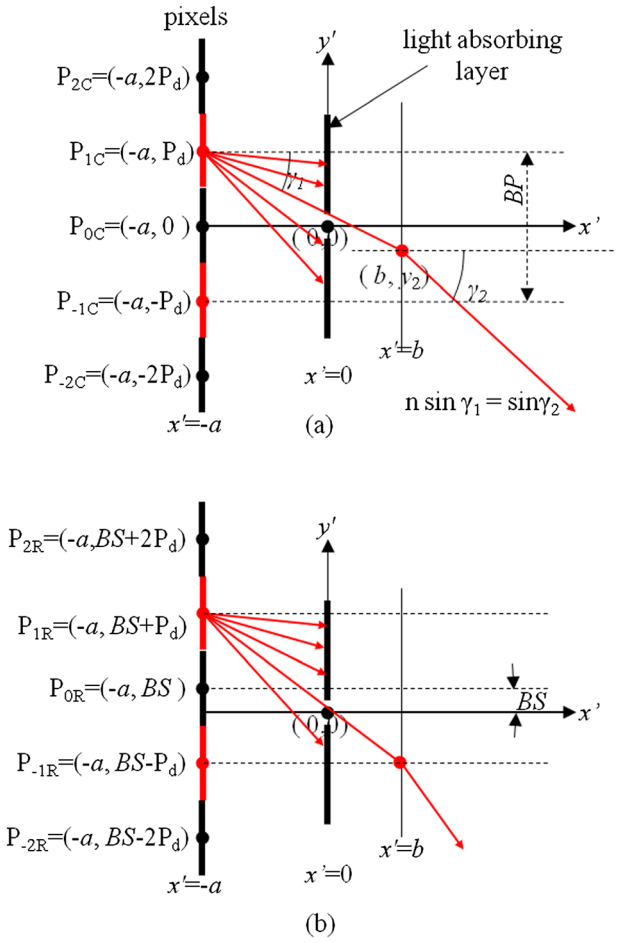

FIGURE 6 — Scheme of the calculation of the ray trajectories coming from pixel $P_{m\mathrm{C}}$ and $P_{m\mathrm{R}}$ through the parallax in the $x'y'$-coordinate system where the x'-axis was normal to the display surface. (a) Ray trajectories at the display center where pixel $P_{0\mathrm{C}}$ and the transparent region of parallax barrier were aligned at the x'-axis. (b) Ray trajectories at the right edge of the display where pixel $P_{0\mathrm{C}}$ was shifted along the direction of the y'-axis by the barrier shift BS compared with the display center. Thick black lines represent the light-absorbing layer of the parallax barrier. m represents the integer of 2, 1, 0, −1, and −2.

The light-absorbing layer of the parallax barrier was selected to be located at $x = 0$, which is represented by black thick lines; (0, 0) of the $x\,y$-coordinate system was selected to be located at the transparent region of the parallax barrier. Five pixels of $P_{2\mathrm{C}} \sim P_{-2\mathrm{C}}$ were located at $x = -a$. The center of pixel $P_{0\mathrm{C}}$ and the transparent region of parallax barrier were selected to be aligned at $y = 0$. Trajectories of the multiple rays coming from the center of each pixel at the xy coordinate of $(-a, mP_d)$ and incident in the range of one barrier pitch were calculated. Integer m was used to represent the five pixels $P_{m\mathrm{C}}$ and $P_{m\mathrm{R}}$ at the center and the right edge of the display in Fig. 6, where m is 2, 1, 0, −1, or −2. Pixels of the odd and even notations corresponded to views for the left or right eyes. At the parallax barrier, the rays incident on the light-absorbing layer were blocked, and the rays incident on the transparent region passed through the substrates. At the boundary between the air and the substrate of the parallax barrier of $x = b$, angle of the ray refracted from γ_1 to γ_2 by Snell's law. Using the information of

the xy-coordinate ($x_2 = b$, y_2) and direction γ_2 at the substrate boundary, the trajectory of each ray in the air was calculated.

The amount of the barrier shift between the pixel center and the transparent region of the barrier determined the viewing distance as illustrated in Figs 2–4. The effect of the barrier shift was applied in the calculation of the ray trajectories by the translation of the pixels coordinates by the amount of the barrier shift BS as illustrated in Fig. 6 (b). M was defined as the number of pixels between the positions of $P_{m\mathrm{C}}$ at the center of the display and $P_{m\mathrm{R}}$ or $P_{m\mathrm{L}}$ at the edge of the display. As $P_{m\mathrm{R}}$ or $P_{m\mathrm{L}}$ was assumed to be located at the horizontal edge of the display at $m = 0$ for the calculation, M was equal to half of the horizontal number of pixels.

In case of autostereoscopic 3D using the flat display, the x y -coordinate system of Fig. 6 was equal to the xy-coordinate system defined in Fig. 2. In that case, BS was equal to BS_f. The distance from the positions of $P_{m\mathrm{C}}$ at the center of the display and to $P_{m\mathrm{R}}$ or $P_{m\mathrm{L}}$ at the edge of the display was $M \times P_d$. Once the information of the xy coordinate (b, y_2) and direction γ_2 at the substrate boundary for $P_{m\mathrm{R}}$ and $P_{m\mathrm{L}}$ were calculated in consideration of the barrier shift BS, trajectories of rays for $P_{m\mathrm{R}}$ and $P_{m\mathrm{L}}$ were obtained by the translation of $(b, y_2 + M \times P_d)$ for $P_{m\mathrm{R}}$ and $(b, y_2 - M \times P_d)$ for $P_{m\mathrm{L}}$ in consideration of the distance $M \times P_d$ from the center of the display to the edge of the display. Calculated trajectories of each ray propagating through the air were represented by the ray direction γ_2 and position (x_3, y_3) at which light ray came out from the substrate of the parallax barrier to the air. In case of pixels at the display center, (x_3, y_3) was equal to (b, y_2), and in case pixels at the display edge, (x_3, y_3) was equal to $(b, y_2 \pm M \times P_d)$.

In the calculation of ray trajectories at the curved surface, the curved display surface can be treated as the flat surface for the range of several pixel sizes on the display surface. Then ray trajectories around the positions of $P_{m\mathrm{C}}$ and $P_{m\mathrm{R}}$ can be calculated by the scheme described in Fig. 6. However, calculated ray trajectories in Fig. 6 were represented in the x y -coordinate system where the x -axis was normal to the display surface. Therefore, the ray trajectories for the pixel at the right edge, calculated by the scheme of Fig. 6(b), should be transformed by the amount derived in Fig. 4(b). Hence, position (x_3, y_3) at which light ray came out from the substrate of the parallax barrier to the air was changed as in Eq. (8a).

$$(x_3, y_3) \Rightarrow (x_3 + \Delta x, y_3 + \Delta y) = (x_3 + R(1 - \cos\phi_2), y_3 - R\sin\phi_2) \tag{8a}$$

And ray directions were changed as in Eq. (8b).

$$\gamma_2 \Rightarrow \gamma_2 + \phi_2 = \gamma_2 + (D_L / R) \tag{8b}$$

Transformation of the information of the ray trajectories in Eqs (8a) and (8b) is illustrated in Fig. 7. Ray trajectories

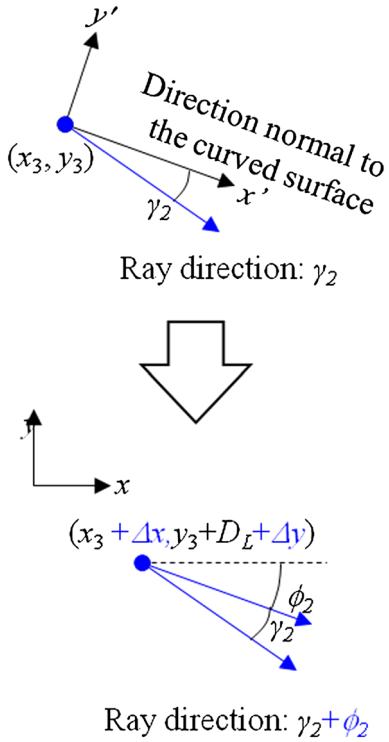

FIGURE 7 — Transformation of ray position and direction from the $x'y'$-coordinate system where the x'-axis was normal to the curved surface to the xy-coordinate system, which was defined with respect to the user position in Figure 4. (x_3, y_3) represents the position at which light ray came out from the substrate of the parallax barrier to the air. γ_2 represents the ray directions.

transformed by Eqs (8a) and (8b) were used to estimate the ray distribution at the user positions.

Spatial distributions of the rays coming through the parallax barrier from pixels located at the center and the right and left edges of the display were derived from the calculated results of (x_3, y_3) and the ray trajectories in the xy-coordinate system. From the spatial distribution of the trajectories, the viewing zones were estimated. Spatial distribution of rays were investigated for three conditions of the display shapes, which were flat surface, the curved surface where the viewing distance was equal to the radius, and the curved surface where the viewing distance was not equal to the radius.

3 Results and analysis

For the flat or curved displays, the trajectories of the rays coming from the autostereoscopic 3D display were calculated by the procedure described earlier.

In case of autostereoscopic two-view 3D of the flat surface, design parameters were determined to be $a = 780\,\mu\mathrm{m}$, $b = 200\,\mu\mathrm{m}$, and $BP_f = 161.7984\,\mu\mathrm{m}$ for the viewing distance of $D = 400\,\mathrm{mm}$ by Eqs (1a)–(4). Figure 8 illustrates the calculated result of ray trajectories. In Fig. 8(a), ten rays with the different angles were set to come out from each center of

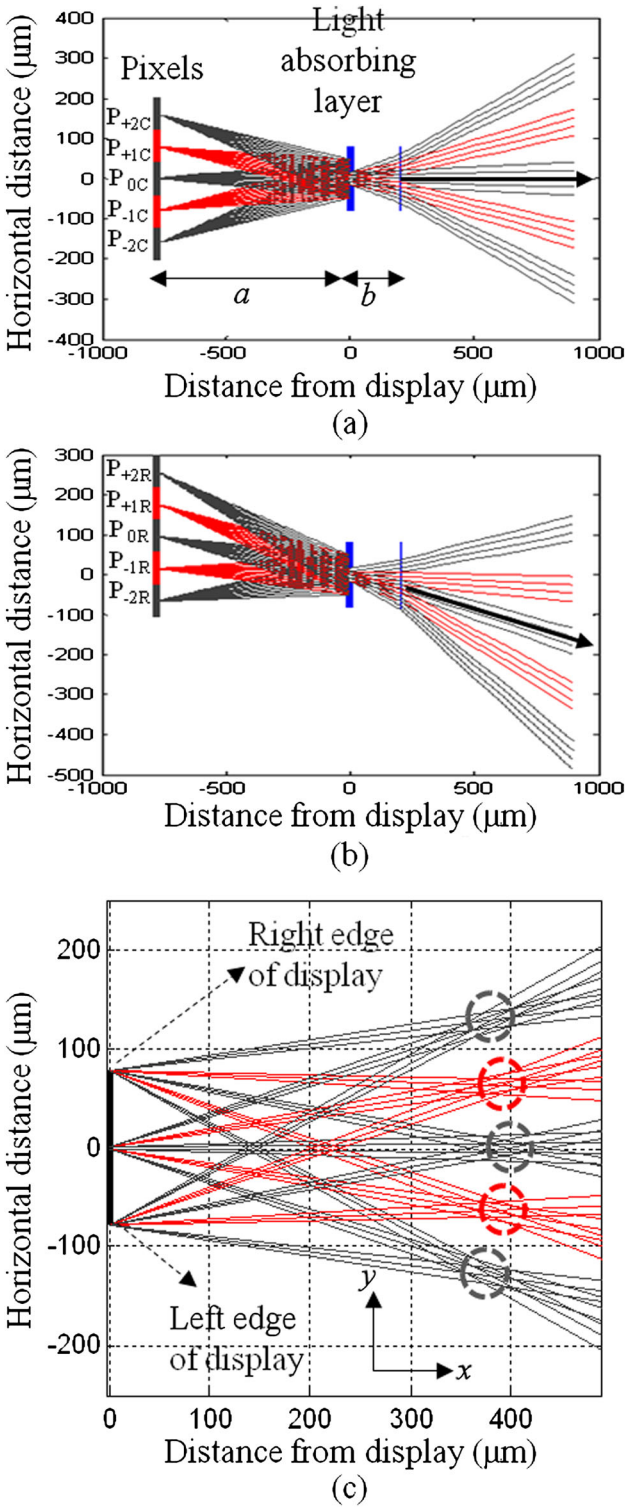

FIGURE 8 — Calculated ray trajectories for autostereoscopic two-view display of the flat surface. (a) Calculated ray trajectories at the center position of the display. (b) Calculated ray trajectories at the right edge of the display. (c) Spatial distribution of the trajectories of the rays coming from the center and the right and left edges of the display. Thick arrows represent the ray coming from P_{0C} or P_{0R} through the transparent region of the parallax barrier. Dotted circles represent the positions where each eye of the viewer should be placed to observe the stereoscopic image. Horizontal axis represents the distance to the user. Vertical axis represents the horizontal distance with respect to the user.

five pixels located at the center position of the display. Some of those rays were blocked at the non-transparent region of the parallax barrier, but three or four rays from each pixel passed through the transparent region of the parallax barrier as illustrated in Fig. 8(a). The number of rays passing through the parallax barrier was determined by the aperture ratio of the parallax barrier. In the calculation of the ray trajectories, the aperture ratio was selected as 0.2. In case of the pixels located at the right edge of the flat display, the barrier shift was 96.78 μm from Eq. 4. The directions of rays passing through the parallax barrier shifted toward the direction of the $-y$-axis as illustrated in Fig. 8(b). The rays coming from the center and the right and left edges of the display intersected at the various positions. The distance from $P_{m\mathrm{C}}$ at the center of the display and to $P_{m\mathrm{R}}$ at the edge of the display was $M \times P_d = 77.8$ mm. In case of ray from the edge of the display, the position of the y-coordinate that the ray came out from the substrate of the parallax barrier to the air was shifted by this distance as explained the calculation scheme of Fig. 6 where at the display edge, (x_3, y_3) was equal to $(b, y_2 \pm M \times P_d)$. Viewing zones were formed where all the rays coming from $P_{m\mathrm{C}}$, $P_{m\mathrm{L}}$, and $P_{m\mathrm{R}}$ intersected. In Fig. 8 (c), the positions that the trajectories intersected were approximately located at the distance of 400 mm, although the intersected position was shorter for the larger horizontal distance from the user position.[7] The distance of 400 mm was equal to the designed viewing distance of $D = 400$ mm. Each eye of a user should be placed at one of these positions to perceive the stereoscopic images.

In case of autostereoscopic two-view 3D where viewing distance D was equal to radius R of the curved display, design parameters were determined to be $a = 780$ μm, $b = 200$ μm, and $BP_r = 161.6849$ μm for the viewing distance of $D = 400$ mm in Eq. (5). The calculated barrier pitch BP_r was calculated to be different for BP_f. Figure 9(a) illustrates the schematic of the calculated ray directions at the center and the right and left edges of the display. In Fig. 9(a), lines connecting the centers of pixels P_{0C}, P_{0L}, and P_{0R} and the transparent region of the parallax barrier were still on the line normal to the display surface, although these lines were no longer parallel to the x-axis. Figure 9(b) illustrates the spatial distribution of the ray trajectories. The positions of intersections of the ray trajectories were approximately at the distance of 400 mm, which was equal to radius R of the curved display.

Figure 10 illustrates the spatial distribution of the calculated ray distribution where radius R of the curved display was not equal to viewing distance D. For the viewing distance of $D = 400$ mm and radius $R = 1.5\ D$ or $2\ D$, design parameters were determined using Eqs 6a, 6b, 7a, 7b, and the calculated ray trajectories were changed by Eqs (8a) and (8b).

Spatial distributions of the ray trajectories of Figs 8(c), 9 (c), and 10 showed the similar trends where the rays from the pixels corresponding to the same view gathered near the distance of 400 mm for the flat display and the curved display of $R = D$, $1.5D$, $2D$.

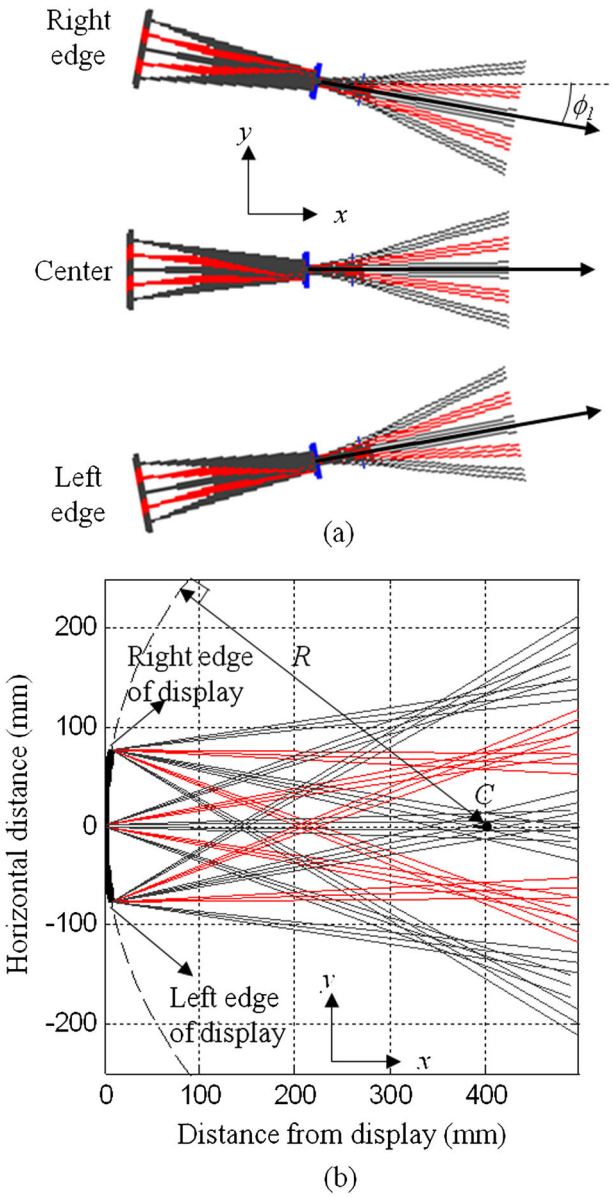

FIGURE 9 — Calculated ray trajectories for autostereoscopic two-view display where radius R is equal to the viewing distance, D. (a) Schematic ray directions at the center and the right and left edges of the display. Thick arrows represent the direction toward the center of the circle composing the circular arc of the concave display. φ_1 represents the angle between the ray trajectories and the x-axis. (b) Spatial distribution of the trajectories of the rays coming from the center and the right and left edges of the display. Thick curve of the left side represents the arc of radius R of the curved display. Horizontal axis represents the distance to the user. Vertical axis represents the horizontal distance with respect to the user. C represents the center of the concave curvature.

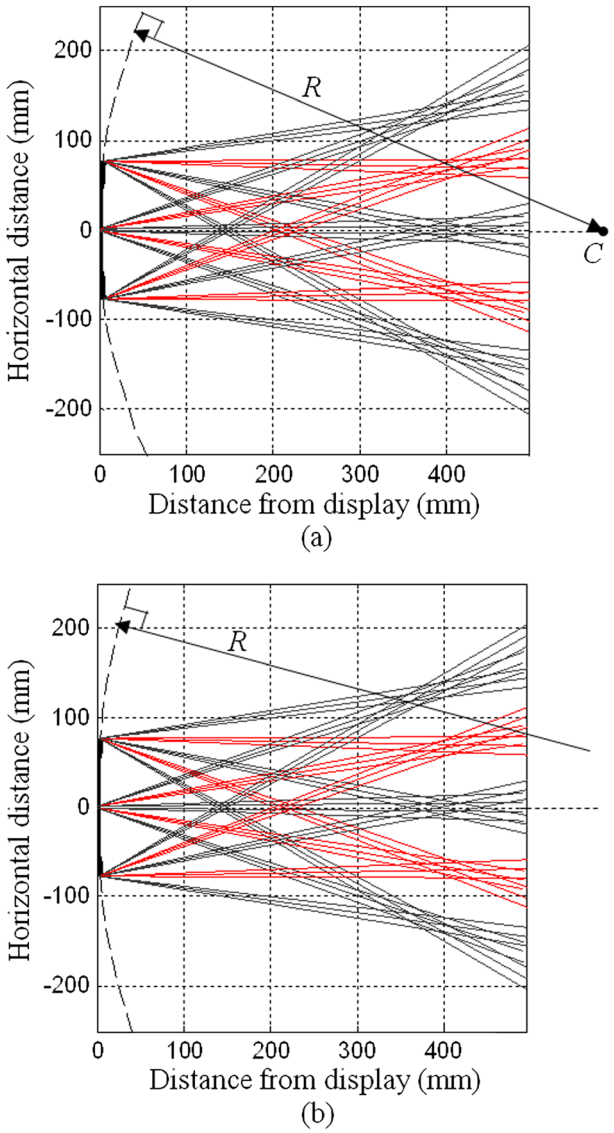

FIGURE 10 — Spatial distribution of the calculated ray trajectories coming from the center and the right and left edges of the curved display for autostereoscopic two-view display where radius R was (a) 1.5D and (b) 2D. Thick curve of the left side represents the arc of radius R of the curved display. Horizontal axis represents the distance to the user. Vertical axis represents the horizontal distance with respect to the user. C represents the center of the concave curvature.

Slight changes of viewing position along the horizontal directions were observed in the calculated results, which had been reported in the flat surface.[7] Hence, once the parameters of the parallax barrier were initially determined by the given equations, optimization of the parameters through calculation of the ray trajectories might be also needed for autostereoscopic 3D using the curved surface. Still, calculated results of the ray trajectories of Figs 9 and 10 for the curved display verify that the designing procedure and the derived equations were useful for designing the autostereoscopic 3D with curved surface.

4 Conclusion

The process for determining the parameter of the parallax barrier was investigated for autostereoscopic 3D with curved surface. Equations of the barrier pitch depending on radius R were derived for the circular concave surface as shown in Table 1. The result showed that equation for the barrier pitch of the flat surface was not applicable to the curved surface and radius R of the curved display should be considered in

designing the parameters for the parallax barrier if the curved display was used.

This research was investigated for autostereoscopic two-view 3D using the parallax barrier. Yet, this investigation is expected to be applicable to autostereoscopic 3D with view number larger than 2. This investigation is also expected to be useful to determine the lens pitch for autostereoscopic 3D using lenticular lens.

Acknowledgment

This research was supported by Basic Science Research Program through the National Research Foundation of Korea (NRF) funded by the Ministry of Education (NRF-2013R1A1A2005812).

References

1 The illustrated 3D movie list, "The illustrated 3D HDTV list", http://www.3dmovielist.com, accessed Feb, 2014.
2 T. Okoshi, "Three dimensional images techniques," New York: Academic Press (1976).
3 C. van Berkel, "Image preparation for 3D-LCD," *Proc. SPIE* **3639**, 84–91 (1999).
4 B. Javidi and F. Okano, "Three-dimensional television, video and display technologies," New York: Springer (2002).
5 J. Y. Son and B. Javidi, "Three-dimensional imaging method based on multiview images," *J. Display Technol.* **1**, 125–140 (2005).
6 H. K. Hong and M. J. Lim, "Determination of luminance distribution of autostereoscopic 3-D displays through calculation of angular profile," *J. SID* **18**, 327–335 (2010).
7 W. H. Hsu *et al.*, "A study of optimal viewing distance in an AS3D display," *SID Digest* **44**, 1198–1201 (2013).
8 J. S. Yoo *et al.*, "Highly flexible AM-OLED display with integrated gate driver using amorphous silicon TFT on ultrathin metal foil," *J. Display Technol.* **6**, 565–570 (2010).
9 J. E. Lee *et al.*, "Flexible display driven by solution-processes OTFTs manufactured using all-sputtered electrodes," *SID Symposium Digest* **44**, 38–40 (2013).
10 D. Hertel, "Viewing direction measurements on flat and curved flexible E-paper displays," *J. SID* **21**, 239–248 (2013).
11 K. C. Heo *et al.*, "Flexible reflective color displays using thermochromic pigments," *J. Opt. Soc. Kor.* **17**, 428–432 (2013).
12 J. C. Heikenfeld, "Flexing and stretching," *Inform. Displays* **29**, 30–34 (2013).
13 Matlab™, www.mathwork.com, accessed Feb 2014.
14 S. H. Kang and H. K. Hong, "In watching 3D stereoscopic display using the binocular disparity, the effect of pupillary distance of adults and children on the perception of 3D image," *J. Korean Oph. Opt. Soc.* **16**, 299–305 (2011).

Hyungki Hong is an assistant professor at the Department of Optometry, Seoul National University of Science and Technology, since 2010 and a member of SID. He received his BS in Physics from Seoul National University and PhD in Physics from Korea Institute of Science and Technology (KAIST). After receiving his PhD in 1998, he joined LG Display (at that time LCD Division of LG Electronics) and worked for the performance improvement and the performance characterization of LCD and 3D display until 2010. He is working for the international standardization of 3D measurement in IEC.